BIOCHEMISTRY
including biophysical chemistry & molecular biology
Article

Biochemistry **2009,** *48,* 9599–9605 9599
DOI: 10.1021/bi901295a

The Cluster of Hydrophobic Residues Controls the Entrance to the Active Site of Choline Oxidase[†]

Yao Xin,[‡] Giovanni Gadda,[‡,§,∥] and Donald Hamelberg*[,‡,∥]

[‡]*Department of Chemistry and* [§]*Department of Biology and* [∥]*The Center for Biotechnology and Drug Design, Georgia State University, Atlanta, Georgia 30302-4098*

Received July 27, 2009; Revised Manuscript Received September 1, 2009

ABSTRACT: The active site of many enzymes is well-protected from solution by a gate. The opening and closing of these gates provide controlled access and could be the rate-limiting steps in catalytic processes. The gating mechanism of an enzyme is therefore very important in gaining broader insight into the entire catalytic process. However, the entrance to active sites and let alone the gating mechanisms are not always obvious from X-ray crystal structures of proteins. Here, we have proposed and quantitatively characterized an alternative gating mechanism controlled by a cluster of hydrophobic residues located on the solvent accessible surface of choline oxidase. We show that the opening and closing of the gate are very fast, and diffusion of choline to the active site is also fast and is partly controlled by the electrostatic potential of the enzyme. Using all-atom molecular dynamics and Brownian dynamics simulations, complete analyses of the mechanism of opening and closing of the gate, the rate of collision of the substrate with the enzyme, and the rate of formation of the complex have been conducted.

The binding of a substrate to the active site of an enzyme is often controlled by two independent processes: the diffusion of the substrate toward the enzyme (*1*) and the gating of the active site, often equivalent to a localized conformational change of a few amino acyl side chains that allows the substrate to reach the active site and form the catalytically relevant enzyme−substrate complex (*2*). The active sites of enzymes are generally well-defined in X-ray crystal structures (*3*). In most cases, X-ray structures also suggest the entrance and gating mechanism of the active site. Over the years, several types of gating mechanisms have been uncovered. These include an open binding pocket with an appreciable amount of solvent accessibility, a fluctuating loop controlling access to the binding site, and a long channel leading to the binding site deep inside the protein (*4*−*10*). A familiar example of one of these cases is the active site of acetylcholinesterase (AChE)[1] that is ∼20 Å deep inside the protein, with the entrance being stochastically controlled by a few residues at the bottom of the "gorge" (*5*, *10*−*12*). When the enzyme is in the opened state, the base of the gorge is wide enough for the substrate to pass through to the active site. When the enzyme is in the closed state, the base of the gorge is narrow enough to keep the substrate away from the active site. Another common example of active site gating is exemplified by β-turn loops controlling access to the active site. For example, HIV-1 protease is a well-known example of an enzyme that controls access to its active site using two β-turn flaps. The two flaps sit directly over the active site and open and close periodically to allow substrate to enter. The gating mechanism of the HIV-1 protease has been the subject of many experimental and theoretical studies (*6*, *13*−*19*).

On the other hand, the entrances to the active sites for many other enzymes are not always obvious from X-ray crystal structures. These static structures do not always represent the ensemble of conformations that allow substrate to enter the active site. The X-ray crystal structure of the resting state of choline oxidase (EC 1.1.3.17, choline-oxygen 1-oxidoreductase) is one such example. In the crystal structure of choline oxidase, the active site is adjacent to a loop and directly underneath a cluster of hydrophobic residues (Met62, Leu65, Val355, Phe357, and Met359), as shown in Figure 1. Choline oxidase catalyzes the oxidation of choline to glycine betaine (*N*,*N*,*N*-trimethylglycine) via two subsequent hydride ion transfer reactions from the alcohol and the enzyme-bound aldehyde intermediate to a flavin cofactor (*20*, *21*). This enzyme is a potential target for developing therapeutic agents against bacteria, which are in need of high levels of glycine betaine to avoid dehydration (*22*, *23*). Choline oxidase has been studied extensively, and a wealth of experimental kinetic data pertaining to the catalytic process is available (*21*, *23*−*26*). According to these studies, the limiting steps for the overall turnover of the enzyme are the two oxidative steps, in which choline is converted to betaine aldehyde and betaine aldehyde to glycine betaine (*21*). Both of these reactions occur on the millisecond time scale, i.e., with rate constants of $\sim 100\ s^{-1}$ at pH 10.0 and 25 °C (*21*). Both substrate binding and the product release processes are extremely fast compared to the catalytic steps, as indicated by a lack of solvent viscosity effects on the k_{cat}/K_m and k_{cat} values with choline as the substrate (*21*).

[†]This work was supported in part by research initiation grants from Georgia State University, the Department of Chemistry, and the Georgia Cancer Coalition (GCC) scholar award to D.H. and a CAREER Award from NSF (MCB-0545712) to G.G.

*To whom correspondence should be addressed: Department of Chemistry, Georgia State University, Atlanta, GA 30303. Telephone: (404) 413-5564. Fax: (404) 413-5551. E-mail: dhamelberg@gsu.edu.

[1]Abbreviations: AChE, acetylcholinesterase; HIV, human immunodeficiency virus; GMC, glucose/methanol/choline; CHO, choline oxidase; MD, molecular dynamics; BD, Brownian dynamics; RESP, Restrained Electrostatic Potential; FAD, flavin adenine dinucleotide; SDA, Simulation of Diffusional Association; APBS, Adaptive Poisson−Boltzmann Solver; rmsd, root-mean-square deviation; PDB, Protein Data Bank.

Published on Web 09/03/2009

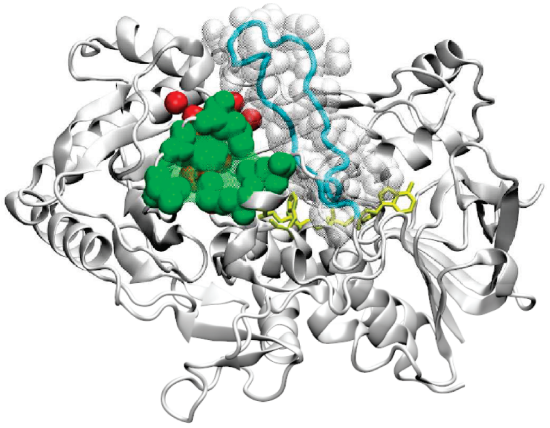

FIGURE 1: Crystal structure of the monomeric form of choline oxidase (PDB entry 2JBV) without substrate bound. The enzyme, with a loop adjacent to the active site (cartoon and transparent VDW, blue), a cluster of hydrophobic residues above the active site (VDW and transparent surface representation, green), water in the active site (VDW, red), and cofactor FAD (licorice, yellow).

However, these two nonchemical processes and the related gating mechanism that contribute to the efficiency of the enzyme are not fully understood.

It is not obvious from the X-ray crystal structure of choline oxidase how choline enters the active site. The gating mechanism is unknown, and several studies on choline oxidase as well as other enzymes belonging to the glucose/methanol/choline (GMC) oxidoreductase enzyme superfamily, of which choline oxidase is a member, have assumed that the entrance is controlled by an extended loop that is adjacent to and covers the active site (*23*, *27*−*30*). For the loop to control the gate to the active site, the time scale of opening and closing has to be significantly faster than the millisecond time scale of the rate-limiting catalytic process, an event that seems unlikely due to the length of the loop (i.e., from residue 74 to 85 in choline oxidase). The time scale of the motion of the loop is not known, and this information is also not evident from the X-ray structure. Understanding this process will provide better insight into the entire catalytic process of choline oxidase and a broader knowledge of enzyme gating. In this regard, we have used all-atom molecular dynamics simulation to probe the atomistic basis for the gating mechanism of choline oxidase.

This work proposes a stochastic gating mechanism that is controlled by side chains of a cluster of hydrophobic amino acids located just above the active site and on the solvent-exposed surface of choline oxidase. We have described the gating mechanism using choline oxidase, but the atomistic basis for the gated process suggests a general mechanism that could also be found close to the surfaces of other enzymes, as observed in gating mechanisms that are used mainly through gorges or channels (*4*, *5*, *9*, *10*, *31*). The simulation results suggest that the gate of choline oxidase is controlled by Met62, Leu65, Val355, Phe357, and Met359. We characterized the opening and closing of the gate; the time scales for both events are fast. Substrate diffusion is also fast and is partly controlled by electrostatic steering that exploits the positive charge harbored on choline.

COMPUTATIONAL METHODS

Molecular Dynamics (*MD*). Two 60 ns molecular dynamics simulations were conducted on free wild-type choline oxidase (CHO) and choline-bound CHO. The initial structure for all the simulations was the only X-ray crystal structure of CHO without the substrate bound (PDB entry 2JBV). CHO was crystallized as a dimer with one active site on each monomer. CHO exists as a homodimer in solution; however, each active site acts independently of the other in experiments, and the sites are ~35 Å from each other. Therefore, we used chain A of the X-ray structure and assumed that chain B has similar properties. To prepare the choline-bound CHO, choline was docked into the active site using AutoDock 4.0 (*32*). Partial charges for every atom of choline are determined by a two-step RESP method (*33*, *34*) based on the grid of electrostatic potential calculated with Gaussian03 (*35*) at the HF/6-31G* level of theory. Molecular dynamics simulations were conducted in explicit TIP3P water using the PMEMD module in Amber 10 (*36*, *37*), the all-atom parm99SB force field (*38*), and GAFF (*39*) parameters for choline. Newton's equation was numerically solved to calculate the forces and update the coordinates of each atom using a time step of 2 fs. A periodic TIP3P truncated octahedral water box was used as the solvent box. We used sodium ions to neutralize the system. All equilibration and production runs were conducted using the NTP (300 K, 1 bar) ensemble. The Langevin thermostat with a collision frequency of 1.0 ps^{-1} for temperature control, the SHAKE algorithm for constraining all bonds involving hydrogens, and particle mesh Ewald summation for evaluating electrostatics interactions with a 9 Å nonbonded cutoff separating the real space from the reciprocal space were also used. To avoid Langevin artifacts (*40*), the random seed was updated every time the simulations were restarted. Snapshots were saved every 500 steps (1.0 ps) for further analyses. We reproduced the covalent linkage between the cofactor flavin adenine dinucleotide (FAD) and His99 as previously described (*23*).

To obtain the time evolution information about the gate opening and closing, each frame was extracted from the last 50 ns MD trajectory and converted to the PDB file format using the PTRAJ module in AMBER, and the Hole program (*41*) was used to determine the minimum pore radius between the active site and the gate formed by the cluster of hydrophobic residues. We set a probe vector and probe point in Hole to force the probe surface to go through the pore. Few negative values were seen, which means that there were few overlaps of the VDW spheres during the calculation of the effective pore radius as previously described (*41*). Only one VDW radius for each element type was used in Hole, compared to several in the AMBER force field. Adaptive Poisson−Boltzmann Solver (APBS) (*42*) was used to generate the electrostatic map of the enzyme by numerically solving the linear Poisson−Boltzmann equation. The grid dimensions were set at 129 Å × 129 Å × 129 Å. Charges and radii for all atoms of the enzyme in the electrostatic calculations were from the AMBER force field. The dielectric constants of grid points representing CHO were assigned to 1 (inside) and 78.5 (outside). Pymol (*43*) was used to visualize the electrostatic map of the open and closed states of the enzyme. VMD (*44*) was used to generate the view of the gate and the active site of the enzyme and also to visualize the MD trajectories.

Brownian Dynamics (*BD*). BD is a powerful tool for calculating diffusional rate constants for biomolecular processes with irregular shape and arbitrary charge distribution. We used Simulation of Diffusional Association (SDA) (*45*−*48*) to conduct the Brownian dynamics simulations. The simulations were conducted with the full electrostatic potential and an additional weak hydrophobic interaction of both the enzyme and the substrate. The effective (potential derived) charges for macromolecules in

solvent (ecm) (*49*) available with SDA were used to evaluate the electrostatic interaction. The low-dielectric substrate and enzyme were considered to be immersed in a uniform high-dielectric solvent with a dielectric constant of 78.5. The effective charges were obtained by fitting them to reproduce the electrostatic potential from solution of the linearized Poisson−Boltzmann equation. The grid dimensions were 129 Å × 129 Å × 129 Å with a spacing of 1 Å. To represent the formation of the enzyme−substrate complex, we used the root-mean-square distance between atoms of the enzyme and the substrate as the reaction criterion. The root-mean-square distance between the nitrogen of choline and the Cα atom of Met62 and the Cα atom of Phe357 of CHO was used as the reaction criterion. Hydrophobic desolvation effect was also included. The relative diffusion coefficient was calculated as the sum of diffusion coefficients of the substrate and enzyme according to $D_{\text{translation}} = \frac{k_B T}{6\pi\eta r}$ The rotational diffusion constants were estimated for both choline and CHO using $D_{\text{rotation}} = \frac{k_B T}{8\pi\eta r^3}$ where k_B is the Boltzmann constant, T is the absolute temperature, η is the solvent viscosity, and r is the hydrodynamic radius of substrate and enzyme, assuming they are effective spheres. The center to center distance at which we started each BD simulation was set to 80 Å, and the simulation was stopped if the distance between the substrate and the enzyme grew to be larger than 160 Å. A total of 10000 trajectories were conducted for each BD simulation to estimate the rate constant. For every different concentration, four independent BD simulations, 10000 trajectories each, were conducted on the basis of different initial random seeds, and the average association rate constant and error were calculated on the basis of the four independent simulations.

RESULTS AND DISCUSSION

The nature of the entrance to active sites of enzymes plays an important role in the catalytic process. The catalytic mechanism of choline oxidase has been extensively characterized experimentally (*21*, *23*−*26*, *50*, *51*). However, little is known about the nonchemical portions of the catalytic process, vis-à-vis, substrate binding and product release. The kinetic studies and X-ray crystal structure of choline oxidase have not been able to provide a conclusive atomistic description of the access to the active site and the ensuing gating mechanism. The rate of formation of the enzyme−substrate complex was shown to be fast and beyond the time scale of the resolution of the experimental techniques that were used to study the chemical processes. Therefore, we have used all-atom molecular dynamics, a simulation tool for studying transient motions of macromolecules, to probe the gating mechanism of choline oxidase. We simulated the free enzyme and the choline-bound complex for 60 ns each and analyzed the last 50 ns, to ensure that the systems were well-equilibrated.

Hydrophobic Gate on the Solvent Accessible Surface. Previously, it had been assumed that the loop adjacent to the active site of choline oxidase, protruding into the bulk solvent and corresponding to residues 74−85, controls the entrance of the substrate to the active site cavity (*21*). The loop, shown in Figure 1, has very limited movement during the entire 60 ns simulation of free choline oxidase, judging from the root-mean-square deviation (rmsd) analysis of the backbone atoms. As one can see in Figure 1, the loop blocks the entrance to the active site, and there is no direct access underneath the loop that leads to the active site. It is therefore unclear how the substrate would gain access to the active site. Experimentally, the only information known is that both substrate binding and product release steps are much faster than the millisecond time scale of the chemical component of the catalytic process, which is fully rate determining for the overall turnover of the enzyme (*21*).

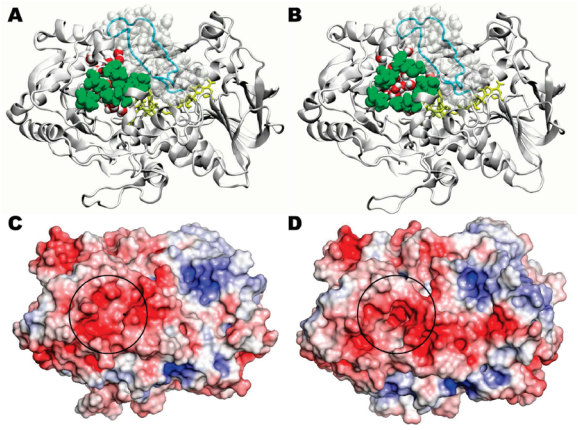

FIGURE 2: Two states of the hydrophobic gate located on the solvent accessible surface of choline oxidase. (A) Closed state. (B) Open state. (C) Electrostatic map of closed state colored by potential on solvent accessible surface with a range from −5 to 5 kT/e. (D) Electrostatic map of the open state. The active site and the gating residue are highlighted by black circles in the electrostatic maps. The loop previously assumed to be the gate to the active site is colored blue. The cofactor FAD covalently linked to His99 is viewed using licorice and is colored yellow. The water molecules at the active site are represented by VDW and colored by element. Our proposed gating residues are colored green using VDW representation.

Further analyses of the trajectory, however, show rapid dynamic motions of a cluster of hydrophobic residues (Met62, Leu65, Val355, Phe357, and Met359) that are located just above the active site on the solvent accessible surface. Some of the conformational transitions or breathing of the side chains was observed to provide openings that allow direct access to the active site from the bulk solvent, as illustrated in Figure 2. We therefore further analyzed the opening and closing of the gate formed by the cluster of hydrophobic residues to investigate whether this finding and time scale are consistent with existing experimental observations. From the frequency of opening and closing and the size of the effective ring formed by the cluster of hydrophobic residues, our results suggest that these five hydrophobic residues control access to the active site from the bulk solvent. In proteins, hydrophobic residues tend to be localized in the core of the protein, away from the solvent accessible surface, to form favorable interactions. This unusual arrangement of the hydrophobic cluster on the solvent accessible surface of choline oxidase may help the positively charged choline efficiently move into the active site. First, the hydrophobic residue will open and close comparatively easier than salt-bridged polar residues to expose the hydrophilic active site. Second, the hydrophobic residues at the gate will not hinder the substrate as it moves into the active site when the substrate is far from the gate or form strong interactions with the substrate as it slips through the gate. The first scenario would happen if the gating residues were positively charged. The second scenario may happen if the gate was negatively charged. Interestingly, the distribution of the residues just outside the five gating residues contains a considerable amount of negatively charged amino acids, which include Glu63, Glu66, Glu358, and Glu370, that may serve to attract and guide the positively charged choline substrate to the active site. This can be clearly seen from the electrostatic map of the closed and open states of the enzyme, also shown in Figure 2 (C and D).

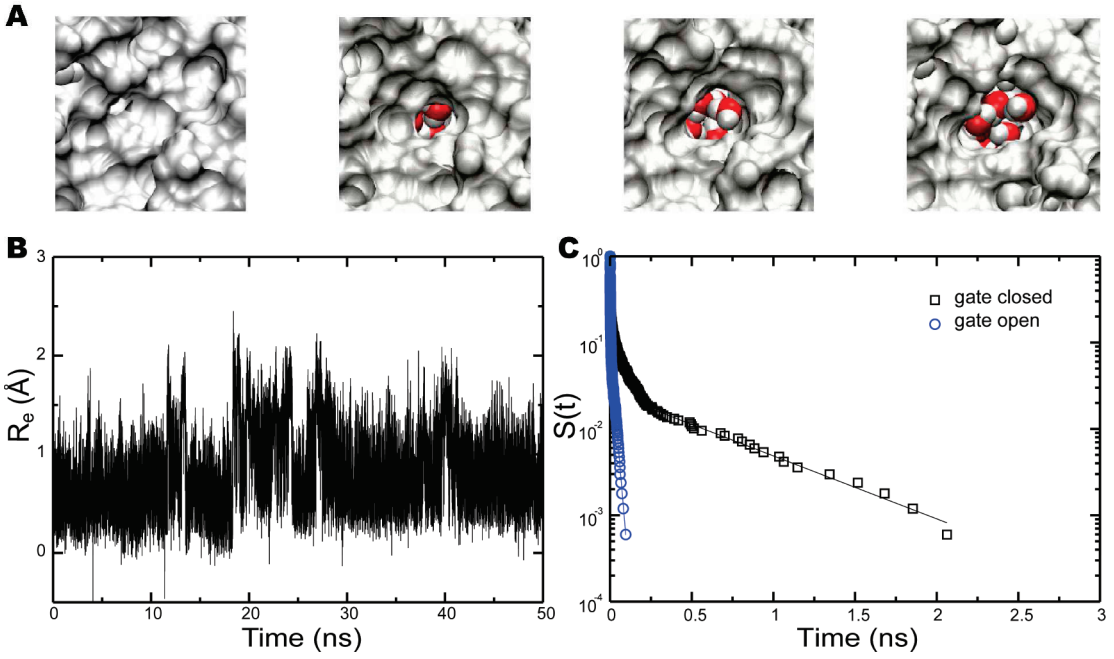

FIGURE 3: Kinetics of the gate to the active site in the free enzyme. (A) Four different conformations with different effective pore radii of 0.0, 1.5, 2.0, and 2.5 Å. The enzyme is represented by a white surface plot, and water molecules in the active site are shown in VDW and colored red and white (A). The view is zoomed to the active site and the proposed gate. (B) Time series of the effective pore radius of the gate. (C) Log plot of the survival functions of the two states: open gate (blue circles), closed gate (black squares), data fitting of the open gate (blue line), and data fitting of the closed gate (black line).

Kinetics of the Gate. To better characterize the kinetics of the gating mechanism that controls access of the substrate to the active site in choline oxidase, we used Hole (*41*) to calculate the minimum effective pore radius between the gating residue and the active site over the entire simulations. Time evolution of the minimum pore radius between the gate and the active site of the free enzyme is shown in Figure 3B. The effective pore radius, R_e, formed by the gating residues fluctuates between 0 and 2.5 Å during the last 50 ns simulation. This clearly shows that the gate controlled by the hydrophobic cluster composed of Met62, Leu65, Val355, Phe357, and Met359 does open and close dynamically. From the electrostatic map shown in Figure 2D, one can see that the active site has a very negative potential that will undoubtedly help to attract the positively charged choline through the gate. The gate was assumed to be open when the effective pore radius is greater than 1.4 Å, the minimum effective pore radius required for the exchange of water molecules between the active site and bulk solvent. A first impression is the rapid transition between gate opening and gate closing on the picosecond time scale. This time scale is also consistent with experiment due to the fact that gating is by far not the rate-determining step for the overall turnover of the enzyme (*21*).

To obtain a more quantitative kinetic description of the opening and closing of the gate, we counted the dwell time (T_i) of opening and closing and then calculated the survival probability distribution from the ordered dwell time (*52*) by $S(t) \approx (i - 1)/N$, where $i = 1, 2, ..., N$, and N is the total number of observed opening to closing transitions. The tail of the log plots of the survival probabilities versus time of the closing and opening events fit to a single exponential, and these give the rate constants of gate closing (k_{close}) and opening (k_{open}), respectively. When there is no substrate bound, the rate constants for gate opening and closing are ~1.7 and ~51.8 ns^{-1}, respectively. This is equivalent to saying that, on average, the gate opens every 595 ps and stays open for 19.3 ps. In Figure 3A, we show four different conformations of the enzymatic gate with different effective pore radii of 0.0, 1.5, 2.0, and 2.5 Å. Clearly from Figure 3, the five hydrophobic residues on the surface form a gating ring that stochastically opens and closes very rapidly.

In the enzyme−substrate complex of choline oxidase, the gate opens slightly wider, with a maximum effective radius of ~3 Å, and stays open slightly longer than in the free enzyme. This suggests that the product leaves the active site of the enzyme the same way the substrate enters. We estimated $k_{open} = 18.0\ ns^{-1}$ and $k_{close} = 11.3\ ns^{-1}$, suggesting that the gate opens every 55.6 ps and stays open for 88.5 ps. The necessity of this increase may come from the slightly larger size of the catalytic product compared to the substrate to efficiently and quickly facilitate product release after catalysis.

Rate of Formation of the Enzyme−Substrate Complex. The rate constant for the association of choline with choline oxidase is too fast to be reliably measured using the techniques that have been used to study the catalytic rates of the chemical processes. The enzyme−substrate complex is fully formed within the time that is required to mix the substrate and enzyme in a stopped-flow spectrophotometer, i.e., ~2 ms (*21*). Also, the electrostatic maps in Figure 2 suggest a possible role of electrostatic steering in guiding choline, which is positively charged, into the active site. Therefore, we have studied the diffusion of choline toward the active site of choline oxidase using Brownian dynamics (BD) simulations to estimate the association rates and probe the role of the electrostatic field of the enzyme. The BD simulations were conducted with an open conformation of the gate of choline oxidase at different salt concentrations. The complex was assumed to be formed when the root-mean-square distance from the nitrogen of choline to two C_α atoms at either side of the entrance of the gate is <8 Å. The distance puts the trimethylammonium group of choline right around the center of the opening. For a salt concentration of 150 mM, the rate constant is ~$1.8 \times 10^9\ M^{-1}\ s^{-1}$, almost at the

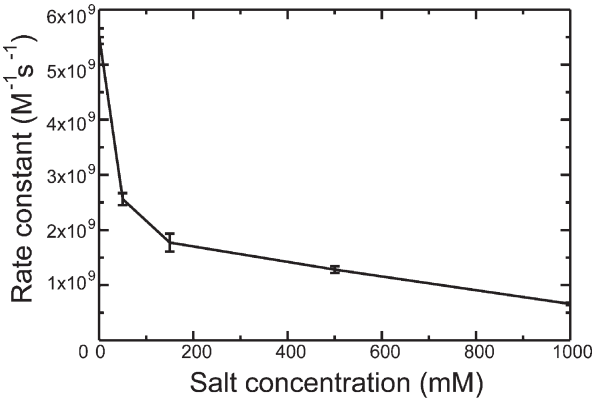

FIGURE 4: Plot of the ionic strength dependence of the rate of formation of the enzyme−substrate complex. The concentration varies from 0 to 1000 mM. The error also shown in the plot is evaluated from four independent simulations based on different initial random seeds.

diffusion-controlled limit (*53*). The rate constants for the association of choline and choline oxidase at five different salt concentrations (0, 50, 150, 500, and 1000 mM) decrease by almost 1 order of magnitude, going from 5.5×10^9 at 0 mM to 6.6×10^8 M^{-1} s^{-1} at 1000 mM, as illustrated in Figure 4. This suggests that the process of forming the complex is at least partly steered by the electrostatics of the enzyme. Also from Figure 4, we see that the electrostatic steering effect is strong at low salt concentrations (i.e., up to and including 150 mM) and is relatively weak at high salt concentrations (i.e., > 500 mM).

The rate of formation of an enzyme−substrate complex involving a stochastic gating mechanism has been extensively studied (*5*, *6*, *54*). The general process is described by eq 1

$$\frac{1}{k_{\text{gated}}} = \frac{1}{k_{\text{ungated}}} + \frac{k_{\text{close}}}{k_{\text{open}}(k_{\text{open}} + k_{\text{close}}) \times \hat{\kappa}_{\text{u}}(k_{\text{open}} + k_{\text{close}})} \quad (1)$$

where k_{gated} is the rate constant of complex formation when the rates of gate opening and closing are taken into consideration and k_{ungated} is the rate constant of complex formation (neglecting the contribution of any gating mechanism) and is equal to the collision rate estimated from the BD simulation. k_{open} is the rate constant for gate opening. k_{close} is the rate constant for gate closing. $\hat{\kappa}_{\text{u}}(k_{\text{open}} + k_{\text{close}})$ is the Laplace transform of the time-dependent rate constant of the ungated protein. The rate of complex formation (k_{gated}) in eq 1 can be simplified on the basis of two limiting cases, i.e., whether the gating mechanism is fast or slow compared to the diffusional relaxation time τ_{d} of the substrate as shown in eq 2 (for slow gating) and eq 3 (for fast gating).

$$k_{\text{gated}} = k_{\text{ungated}} \frac{k_{\text{open}}}{k_{\text{close}} + k_{\text{open}}} \qquad (k_{\text{open}} + k_{\text{close}})^{-1} \gg \tau_{\text{d}} \quad (2)$$

$$k_{\text{gated}} = k_{\text{ungated}} \qquad (k_{\text{open}} + k_{\text{close}})^{-1} \ll \tau_{\text{d}} \quad (3)$$

In this study, $(k_{\text{open}} + k_{\text{close}})^{-1}$ is in the same order of magnitude as τ_{d}, the diffusional relaxation time of choline. Therefore, we can conclude that rate of formation of the enzyme−substrate complex (k_{gated}) is in the range of 10^7−10^9 M^{-1} s^{-1}.

Choline oxidase is a homodimer in solutions, with two active sites ~35 Å from each other. Experimentally, it has been shown that these two identical active sites act in a manner independent of each other. Therefore, to reduce the complexity of the system, we conducted the simulations using a single monomer. Since the two independent active sites are far from each other and the entrances are on the solvent accessible surface, we do not expect dimerization to drastically affect the kinetics of binding. Recent studies by Gorfe et al. (*55*) on the effect of oligomerization of acetylcholinesterase on the rate of ligand binding show that the relative motions of the monomers in an oligomeric enzyme reduce the effect of oligomerization. They concluded that the dynamics of the system allows the enzyme to maintain a similar efficiency in different oligomerization states.

In conclusion, the gating of the active site of an enzyme and the rate of formation of the enzyme−substrate complex are very important for the catalytic process, because the gating mechanism, being kinetically equivalent to a first-order isomerization step between two enzyme−substrate conformations with rate constants of interconversion that are independent of the concentration of substrate, could be the rate-limiting step and define the overall rate of turnover of the enzyme. In this work, we have proposed a gating mechanism for choline oxidase that is different from that previously proposed in several studies of this enzyme and other members of the GMC oxidoreductase enzyme superfamily that have assumed that the entrance is controlled by an extended loop adjacent to the active site. We have quantitatively characterized by all-atom molecular dynamics and Brownian dynamics simulations a hydrophobic gating "ring" located on the solvent accessible surface of choline oxidase. The gating is shown to occur mainly through hydrophobic interactions among a cluster of the side chain of five residues (Met62, Leu65, Val355, Phe357, and Met359). These residues form a gate that opens and closes and provides direct access to the active site. The weakly hydrophobic interactions between the gating residues ensure that the positively charged substrate can easily slip to the highly electronegative active site. The efficiency of this novel gating mechanism can be seen from comprehensive analyses of the kinetic data. The results show that the transition between gate opening and closing is rapid and occurs on the picosecond time scale. The rate of complex formation was estimated from the rate of diffusion of the substrate toward the active site. This work supports and complements previously drawn conclusions from experiments (*21*) that the formation of the enzyme−substrate complex and the release of the product of the reaction of oxidation of choline catalyzed by choline oxidase are very fast, compared to the chemical steps of the enzymatic process. We have shed light on the gating mechanism of choline oxidase at the atomistic level of detail that might provide insight into manipulating the catalytic process through enzyme engineering and mutagenesis studies. We expect that similar mechanisms in which access of the organic substrate to the active site is gated by a cluster of hydrophobic amino acyl residues and the associated kinetic properties would be found in other enzymes, either in different locations of the enzyme or in slightly different gating residues (*4*, *9*, *31*), especially in the GMC oxidoreductase enzyme superfamily of enzymes (*27*−*30*).

ACKNOWLEDGMENT

We acknowledge computer time at Georgia State's IBM System p5 supercomputer, acquired through a partnership of the Southeastern Universities Research Association and IBM supporting the SURAgrid initiative.

REFERENCES

1. Allison, S. A., Northrup, S. H., and McCammon, J. A. (1986) Simulation of biomolecular diffusion and complex formation. *Biophys. J. 49*, 167–175.
2. McCammon, J. A., and Northrup, S. H. (1981) Gated binding of ligands to proteins. *Nature 293*, 316–317.
3. Carlson, H. A., Smith, R. D., Khazanov, N. A., Kirchhoff, P. D., Dunbar, J. B., Jr., and Benson, M. L. (2008) Differences between high- and low-affinity complexes of enzymes and nonenzymes. *J. Med. Chem. 51*, 6432–6441.
4. Murray, L. J., Garcia-Serres, R., McCormick, M. S., Davydov, R., Naik, S. G., Kim, S. H., Hoffman, B. M., Huynh, B. H., and Lippard, S. J. (2007) Dioxygen activation at non-heme diiron centers: Oxidation of a proximal residue in the I100W variant of toluene/o-xylene monooxygenase hydroxylase. *Biochemistry 46*, 14795–14809.
5. Zhou, H. X., Wlodek, S. T., and McCammon, J. A. (1998) Conformation gating as a mechanism for enzyme specificity. *Proc. Natl. Acad. Sci. U.S.A. 95*, 9280–9283.
6. Chang, C. E., Shen, T., Trylska, J., Tozzini, V., and Mccammon, J. A. (2006) Gated binding of ligands to HIV-1 protease: Brownian dynamics simulations in a coarse-grained model. *Biophys. J. 90*, 3880–3885.
7. Hritz, J., Zoldak, G., and Sedlak, E. (2006) Cofactor assisted gating mechanism in the active site of NADH oxidase from *Thermus thermophilus*. *Proteins 64*, 465–476.
8. Kato, M., Wynn, R. M., Chuang, J. L., Brautigam, C. A., Custorio, M., and Chuang, D. T. (2006) A synchronized substrate-gating mechanism revealed by cubic-core structure of the bovine branched-chain α-ketoacid dehydrogenase complex. *EMBO J. 25*, 5983–5994.
9. Murray, L. J., and Lippard, S. J. (2007) Substrate trafficking and dioxygen activation in bacterial multicomponent monooxygenases. *Acc. Chem. Res. 40*, 466–474.
10. Shen, T. Y., Tai, K., and McCammon, J. A. (2001) Statistical analysis of the fractal gating motions of the enzyme acetylcholinesterase. *Phys. Rev. E 63*, 041902.
11. Xu, Y., Shen, J., Luo, X., Silman, I., Sussman, J., Chen, K., and Jiang, H. (2003) How does Huperzine A Enter and Leave the Binding Gorge of Acetylcholinesterase? Steered Molecular Dynamics Simulations. *J. Am. Chem. Soc. 125*, 11340–11349.
12. Niu, C., Xu, Y., Xu, Y., Luo, X., Duan, W., Silman, I., Sussman, J., Zhu, W., Chen, K., Shen, J., and Jiang, H. (2005) Dynamic Mechanism of E2020 Binding to Acetylcholinesterase: A Steered Molecular Dynamics Simulation. *J. Phys. Chem. B 109*, 23730–23738.
13. Hornak, V., Okur, A., Rizzo, R. C., and Simmerling, C. (2006) HIV-1 protease flaps spontaneously close to the correct structure in simulations following manual placement of an inhibitor into the open state. *J. Am. Chem. Soc. 128*, 2812–2813.
14. Galiano, L., Ding, F., Veloro, A. M., Blackburn, M. E., Simmerling, C., and Fanucci, G. E. (2009) Drug pressure selected mutations in HIV-1 protease alter flap conformations. *J. Am. Chem. Soc. 131*, 430–431.
15. Liu, F., Kovalevsky, A. Y., Louis, J. M., Boross, P. I., Wang, Y. F., Harrison, R. W., and Weber, I. T. (2006) Mechanism of drug resistance revealed by the crystal structure of the unliganded HIV-1 protease with F53L mutation. *J. Mol. Biol. 358*, 1191–1199.
16. Hamelberg, D., and McCammon, J. A. (2005) Fast peptidyl cis-trans isomerization within the flexible Gly-rich flaps of HIV-1 protease. *J. Am. Chem. Soc. 127*, 13778–13779.
17. Ishima, R., Wingfield, P. T., Stahl, S. J., Kaufman, J. D., and Torchia, D. A. (1998) Using amide H-1 and N-15 transverse relaxation to detect millisecond time-scale motions in perdeuterated proteins: Application to HIV-1 protease. *J. Am. Chem. Soc. 120*, 10534–10542.
18. Torbeev, V. Y., Raghuraman, H., Mandal, K., Senapati, S., Perozo, E., and Kent, S. B. (2009) Dynamics of "flap" structures in three HIV-1 protease/inhibitor complexes probed by total chemical synthesis and pulse-EPR spectroscopy. *J. Am. Chem. Soc. 131*, 884–885.
19. Hornak, V., Okur, A., Rizzo, R. C., and Simmerling, C. (2005) HIV-1 protease flaps spontaneously open and reclose in molecular dynamics simulations. *Proc. Natl. Acad. Sci. U.S.A. 103*, 915–920.
20. Ikuta, S., Imamura, S., Misaki, H., and Horiuti, Y. (1977) Purification and characterization of choline oxidase from *Arthrobacter globiformis*. *J. Biochem. 82*, 1741–1749.
21. Fan, F., and Gadda, G. (2005) On the catalytic mechanism of choline oxidase. *J. Am. Chem. Soc. 127*, 2067–2074.
22. O'Callaghan, J., and Condon, S. (2000) Growth of *Lactococcus lactis* strains at low water activity: Correlation with the ability to accumulate glycine betaine. *Int. J. Food Microbiol. 55*, 127–131.
23. Quaye, O., Lountos, G. T., Fan, F., Orville, A. M., and Gadda, G. (2008) Role of Glu312 in binding and positioning of the substrate for the hydride transfer reaction in choline oxidase. *Biochemistry 47*, 243–256.
24. Orville, A. M., Lountos, G. T., Finnegan, S., Gadda, G., and Prabhakar, R. (2009) Crystallographic, spectroscopic, and computational analysis of a flavin C4a-oxygen adduct in choline oxidase. *Biochemistry 48*, 720–728.
25. Gadda, G., Fan, F., and Hoang, J. V. (2006) On the contribution of the positively charged headgroup of choline to substrate binding and catalysis in the reaction catalyzed by choline oxidase. *Arch. Biochem. Biophys. 451*, 182–187.
26. Ghanem, M., and Gadda, G. (2006) Effects of reversing the protein positive charge in the proximity of the flavin N(1) locus of choline oxidase. *Biochemistry 45*, 3437–3447.
27. Hecht, H. J., Kalisz, H. M., Hendle, J., Schmid, R. D., and Schomburg, D. (1993) Crystal Structure of Glucose Oxidase from *Aspergillus niger* Refined at 2.3 Angstrom Resolution. *J. Mol. Biol. 229*, 153–172.
28. Hallberg, B. M., Leitner, C., Haltrich, D., and Divne, C. (2004) Crystal structure of the 270 kDa homotetrameric lignin-degrading enzyme pyranose 2-oxidase. *J. Mol. Biol. 341*, 781–796.
29. Bannwarth, M., Bastian, S., Heckmann-Pohl, D., Giffhorn, F., and Schulz, G. E. (2004) Crystal structure of pyranose 2-oxidase from the white-rot fungus *Peniophora* sp. *Biochemistry 43*, 11683–11690.
30. Hallberg, B. M., Henriksson, G., Pettersson, G., and Divne, C. (2002) Crystal structure of the flavoprotein domain of the extracellular flavocytochrome cellobiose dehydrogenase. *J. Mol. Biol. 315*, 421–434.
31. Schwab, F., van Gunsteren, W. F., and Zagrovic, B. (2008) Computational study of the mechanism and the relative free energies of binding of anticholesteremic inhibitors to squalene-hopene cyclase. *Biochemistry 47*, 2945–2951.
32. Morris, G. M., Goodsell, D. S., Halliday, R. S., Huey, R., Hart, W. E., Belew, R. K., and Olson, A. J. (1998) Automated docking using a Lamarckian genetic algorithm and an empirical binding free energy function. *J. Comput. Chem. 19*, 1639–1662.
33. Bayly, C. I., Cieplak, P., Cornell, W. D., and Kollman, P. A. (1993) A Well-Behaved Electrostatic Potential Based Method Using Charge Restraints for Deriving Atomic Charges: The Resp Model. *J. Phys. Chem. 97*, 10269–10280.
34. Cornell, W. D., Cieplak, P., Bayly, C. I., and Kollman, P. A. (1993) Application of Resp Charges to Calculate Conformational Energies, Hydrogen-Bond Energies, and Free-Energies of Solvation. *J. Am. Chem. Soc. 115*, 9620–9631.
35. Frisch, M. J., Trucks, G. W., Schlegel, H. B., Scuseria, G. E., Robb, M. A., Cheeseman, J. R., Montgomery, J., Jr., Vreven, T., Kudin, K. N., Burant, J. C., Millam, J. M., Iyengar, S. S., Tomasi, J., Barone, V., Mennucci, B., Cossi, M., Scalmani, G., Rega, N., Petersson, G. A., Nakatsuji, H., Hada, M., Ehara, M., Toyota, K., Fukuda, R., Hasegawa, J., Ishida, M., Nakajima, T., Honda, Y., Kitao, O., Nakai, H., Klene, M., Li, X., Knox, J. E., Hratchian, H. P., Cross, J. B., Bakken, V., Adamo, C., Jaramillo, J., Gomperts, R., Stratmann, R. E., Yazyev, O., Austin, A. J., Cammi, R., Pomelli, C., Ochterski, J. W., Ayala, P. Y., Morokuma, K., Voth, G. A., Salvador, P., Dannenberg, J. J., Zakrzewski, V. G., Dapprich, S., Daniels, A. D., Strain, M. C., Farkas, O., Malick, D. K., Rabuck, A. D., Raghavachari, K., Foresman, J. B., Ortiz, J. V., Cui, Q., Baboul, A. G., Clifford, S., Cioslowski, J., Stefanov, B. B., Liu, G., Liashenko, A., Piskorz, P., Komaromi, I., Martin, R. L., Fox, D. J., Keith, T., Al-Laham, M. A., Peng, C. Y., Nanayakkara, A., Challacombe, M., Gill, P. M. W., Johnson, B., Chen, W., Wong, M. W., Gonzalez, C., and Pople, J. A. (2004) Gaussian 03 , revision E.01, Gaussian, Inc., Wallingford, CT.
36. Case, D. A., Cheatham, T. E.III, Darden, T., Gohlke, H., Luo, R., Merz, K. M., Jr., Onufriev, A., Simmerling, C., Wang, B., and Woods, R. J. (2005) The Amber biomolecular simulation programs. *J. Comput. Chem. 26*, 1668–1688.
37. Case, D. A., Darden, T. A., Cheatham, T. E., III, Simmerling, C. L., Wang, J., Duke, R. E., Luo, R., Crowly, M., Walker, R. C., Zhang, W., Merz, K. M., Wang, B., Hayik, S., Roitberg, A., Seabra, G., Kolossváry, I., Wong, K. F., Pasani, F., Vanicek, J., Wu, X., Brozell, S. R., Steinbrecher, T., Gohlke, H., Yang, L., Tan, C., Mongan, J., Hornak, V., Cui, G., Mathews, D. H., Seetin, M. G., Sagui, C., Babin, V., and Kollman, P. A. (2008) AMBER 10 , University of California, San Fransisco.
38. Hornak, V., Abel, R., Okur, A., Strockbine, B., Roitberg, A., and Simmerling, C. (2006) Comparison of multiple Amber force fields and development of improved protein backbone parameters. *Proteins 65*, 712–725.
39. Wang, J., Wolf, R. M., Caldwell, J. W., Kollman, P. A., and Case, D. A. (2004) Development and testing of a general amber force field. *J. Comput. Chem. 25*, 1157–1174.

40. Cerutti, D. S., Duke, R., Freddolino, P. L., Fan, H., and Lybrand, T. P. (2008) Vulnerability in Popular Molecular Dynamics Packages Concerning Langevin and Andersen Dynamics. *J. Chem. Theory Comput. 4*, 1669–1680.
41. Smart, O. S., Goodfellow, J. M., and Wallace, B. A. (1993) The pore dimensions of gramicidin A. *Biophys. J. 65*, 2455–2460.
42. Baker, N. A., Sept, D., Joseph, S., Holst, M. J., and McCammon, J. A. (2001) Electrostatics of nanosystems: Application to microtubules and the ribosome. *Proc. Natl. Acad. Sci. U.S.A. 98*, 10037–10041.
43. Warren, L. (2007) The PyMOL Molecular Graphics System , DeLano Scientific LLC, San Carlos, CA.
44. Humphrey, W., Dalke, A., and Schulten, K. (1996) VMD: Visual molecular dynamics. *J. Mol. Graphics 14*, 27–38.
45. Gabdoulline, R. R., and Wade, R. C. (1997) Simulation of the diffusional association of barnase and barstar. *Biophys. J. 72*, 1917–1929.
46. Gabdoulline, R. R., and Wade, R. C. (1998) Brownian dynamics simulation of protein-protein diffusional encounter. *Methods 14*, 329–341.
47. Gabdoulline, R. R., and Wade, R. C. (1999) On the protein-protein diffusional encounter complex. *J. Mol. Recognit. 12*, 226–234.
48. Elcock, A. H., Gabdoulline, R. R., Wade, R. C., and McCammon, J. A. (1999) Computer simulation of protein-protein association kinetics: Acetylcholinesterase-fasciculin. *J. Mol. Biol. 291*, 149–162.
49. Gabdoulline, R. R., and Wade, R. C. (1996) Effective charges for macromolecules in solvent. *J. Phys. Chem. 100*, 3868–3878.
50. Ghanem, M., and Gadda, G. (2005) On the catalytic role of the conserved active site residue His466 of choline oxidase. *Biochemistry 44*, 893–904.
51. Rungsrisuriyachai, K., and Gadda, G. (2008) On the role of histidine 351 in the reaction of alcohol oxidation catalyzed by choline oxidase. *Biochemistry 47*, 6762–6769.
52. Hamelberg, D., Shen, T., and McCammon, J. A. (2005) Relating kinetic rates and local energetic roughness by accelerated molecular-dynamics simulations. *J. Chem. Phys. 122*, 241103.
53. McCammon, J. A., and Harvey, S. C. (1987) Dynamics of proeins and nucleic acids , University of Cambridge Press, Cambridge, U.K.
54. Zhou, H. X. (1998) Theory of the diffusion-influenced substrate binding rate to a buried and gated active site. *J. Chem. Phys. 108*, 8146–8154.
55. Gorfe, A. A., Lu, B., Yu, Z., and McCammon, J. A. (2009) Enzymatic Activity versus Structural Dynamics: The Case of Acetylcholinesterase Tetramer. *Biophys. J. 97*, 897–905.